

# Techniques to Study Spectral Properties of the Robin-Schwarz Operator at the Continuous Level

Daniel Bennequin, François Cuvelier<sup>[0009-0002-0792-521X]</sup>,  
Martin J. Gander<sup>[0000-0001-8450-9223]</sup>, and Laurence Halpern<sup>[0000-0002-7877-7130]</sup>

## 1 Introduction

In the context of multilevel domain decomposition methods, we are interested in understanding the iteration process for Schwarz domain decomposition methods in the presence of cross points. In the short proceedings manuscript [2], we investigated for the first time directly which error components remain in classical and optimized Schwarz methods, and identified them with the eigenfunctions of the Schwarz iteration operator with eigenvalues close to 1.

It is therefore of interest to understand the spectral properties of the Schwarz iteration operator. General results are known for operators with specific properties, like self-adjoint and/or compact operators. For instance, when discretizing the Laplace equation with finite elements, the variational formulation produces a symmetric and positive definite matrix, and the convergence properties of iterative methods like Jacobi or Conjugate Gradients can be derived from the knowledge of the eigenvalues of this matrix, see [9].

When using more sophisticated iterative methods of domain decomposition type, the subproblems in the subdomains inherit the same symmetry and positivity properties from the global operator, the Laplacian in our case, but the domain decomposition iteration operator might have different properties depending on the domain decomposition method used. The additive Schwarz method leads to a preconditioner that is also symmetric and positive definite in the Laplace case, see [5] for an analysis at the

---

Daniel Bennequin  
Université Sorbonne Paris Cité, e-mail: bennequin@math.univ-paris-diderot.fr

François Cuvelier  
Université Sorbonne Paris Nord, e-mail: cuvelier@math.univ-paris13.fr

Martin J. Gander  
Université de Genève, e-mail: martin.gander@unige.ch

Laurence Halpern  
Université Sorbonne Paris Nord, e-mail: halpern@math.univ-paris13.fr

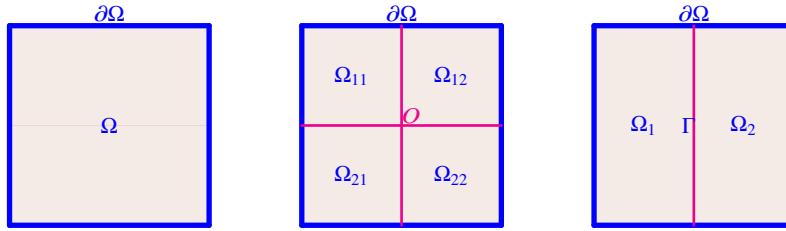


**Fig. 1** Model geometry and domain decompositions with and without cross point.

continuous level, but it is different from the parallel Schwarz method introduced by Lions [6] which solves on all overlapping subdomains in parallel and then exchanges Dirichlet data with neighbors. It is Restricted Additive Schwarz that represents a discretization of Lions' parallel Schwarz method [4], but it is also non-symmetric like Lions' method, even for the Laplace problem. Symmetry is also lost when using other transmission conditions, for example of Robin type, also introduced by Lions to obtain non-overlapping Schwarz methods [7].

We present here for the first time for the Laplace problem and four square subdomains (see Figure 1 middle), the tools and techniques needed to obtain a complete description of the spectral properties of the Schwarz iteration map when using Robin transmission conditions and no overlap, as introduced by Lions in [7].

## 2 The Robin-Schwarz operator

Using the non-overlapping parallel Schwarz method of Lions with Robin transmission conditions [7], the solution  $u$  of the Poisson problem  $-\Delta u = f$  in the domain  $\Omega := (-H, H) \times (-H, H)$  (see Figure 1 left) with zero boundary conditions,  $u = 0$  on  $\partial\Omega$ , is computed as the limit of the sequence of solutions of the same problem in the subdomains  $\Omega_{ij}$  (see Figure 1 middle), with Robin transmission conditions with real positive parameter  $p$  on the interfaces,

$$\begin{aligned} -\Delta u_{ij}^n &= f && \text{in } \Omega_{ij}, \\ u_{ij}^n &= 0 && \text{on } \partial\Omega \cap \partial\Omega_{ij}, \\ \partial_{\nu_{ij}} u_{ij}^n + p u_{ij}^n &= \partial_{\nu_{i\tilde{j}}} u_{i\tilde{j}}^{n-1} + p u_{i\tilde{j}}^{n-1} && \text{on } \partial\Omega_{ij} \cap \partial\Omega_{i\tilde{j}}. \end{aligned} \quad (1)$$

Here,  $\partial\Omega_{ij}$  denotes the boundary of  $\Omega_{ij}$ , the index  $i\tilde{j}$  the corresponding neighboring subdomain of  $ij$ , and we will use  $\partial\Omega_{ij}$  to denote the internal boundary of  $\Omega_{ij}$  equal to  $\partial\Omega_{ij} \setminus \partial\Omega$ . We define the function space

$$\mathbb{U} := \left\{ \mathbf{u} = (u_{11}, u_{12}, u_{21}, u_{22}) \in \Pi_{i,j} H^{\frac{3}{2}}(\Omega_{ij}), -\Delta u_{ij} = 0 \text{ in } \Omega_{ij}, u_{ij} = 0 \text{ on } \partial\Omega_{ij} \cap \partial\Omega \right\}. \quad (2)$$

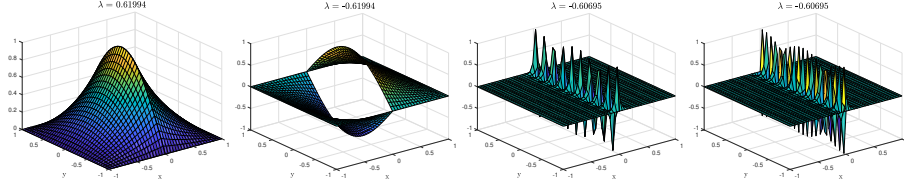


**Fig. 2** Two subdomains. From left to right: continuous and discontinuous eigenmodes for  $k = 1$ , and continuous and discontinuous eigenmodes for  $k = 19$ .

The Robin-Schwarz iteration operator with parameter  $p$  is defined by

$$\mathcal{T} : \mathbf{u} \in \mathbb{U} \rightarrow \mathbf{v} \in \mathbb{U} \quad \text{with} \quad \partial_{\nu_{ij}} v_{ij} + p v_{ij} = \partial_{\nu_{ij}} u_{\bar{i}\bar{j}} + p u_{\bar{i}\bar{j}} \quad \text{on} \quad \partial\Omega_{ij} \cap \partial\Omega_{\bar{i}\bar{j}}. \quad (3)$$

It can be proved that  $\mathcal{T}$  is continuous in  $\mathbb{U}$ . A crucial observation is that on each subdomain  $\Omega_{ij}$ , the trace  $\gamma u_{ij} \in H_0^1(\partial\Omega_{ij})$ , which transfers the analysis from  $\mathbb{U}$  to  $(H^1(0, H))^2$  with compatibility condition (space  $W$  below). Here is the outline on the study of the spectrum of  $\mathcal{T}$ :

1. Identification of those eigenvalues and eigenfunctions of  $\mathcal{T}$  obtained by separation of variables.
2. Association of the eigenfunctions with the special functions  $\sin \zeta_k x \sinh \zeta_k y$ .
3. Study of the dispersion equation and counting of the eigenvalues.
4. Prove that the  $\sin \zeta_k x$  form Schauder or Riesz bases.
5. Study the operator  $\mathcal{A}$  that maps the  $\sin \zeta_k x$  to the  $\sinh \zeta_k x$ .
6. Define a proper operator  $\mathcal{B}$  to treat  $\mathcal{T}$  on the boundary of the subdomain.
7. Deduce the density of the traces of the eigenmodes from item 1.
8. Finally characterize the complete spectrum.

### 3 Eigenvalues and Eigenfunctions by separation of variables

In [2], we studied how to find  $(\lambda, \mathbf{u})$  with  $\mathbf{u} \neq 0$  such that  $\mathcal{T}\mathbf{u} = \lambda\mathbf{u}$  by separation of variables. For 2 subdomains (see Figure 1 right) this can be done by Hilbert analysis. Since the sequence  $\varphi_k(y) = \sin \alpha_k(y + H)$ ,  $\alpha_k = \frac{\pi}{2H}$ , for  $k \geq 1$  is a Hilbert basis in  $H_0^1(\Gamma)$ ,  $\Gamma = (-H, H)$ , the modes can be written as  $\mathbf{u} = (u_1, u_2)$ ,

$$u_1 = a_1 \sinh \alpha_k(x + H) \varphi_k(y), \quad u_2 = a_2 \sinh \alpha_k(x - H) \varphi_k(y),$$

which makes the spectral analysis easy. For each frequency  $k$ , there are two opposite real eigenvalues, and two eigenmodes, one is continuous along the interface, and the other discontinuous. We show in Figure 2 the modes corresponding to the lowest frequency,  $k = 1$  and to a high frequency  $k = 19$ , with  $H = 1$  and  $p = 7.3$ . We will next see that the determination of a basis of eigenmodes is much more involved with a cross-point.

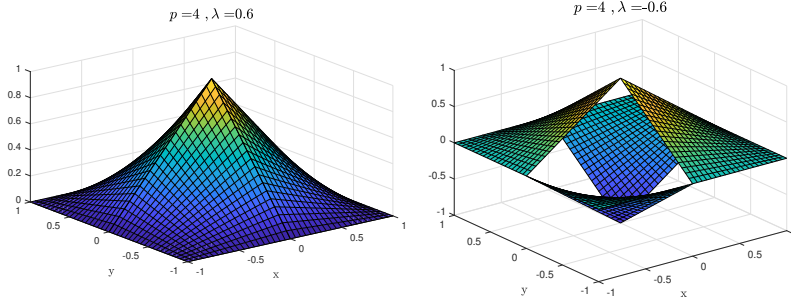


**Fig. 3** Continuous and discontinuous affine modes in the presence of a cross point.

### 3.1 Cross-point case: bi-affine modes

In the case with a cross-point (see Figure 1 middle), there are bi-affine modes of the form

$$\begin{aligned} u_{11} &= a_{11}(x+H)(y-H), & u_{12} &= a_{12}(x-H)(y-H), \\ u_{21} &= a_{21}(x+H)(y+H), & u_{22} &= a_{22}(x-H)(y+H). \end{aligned} \quad (4)$$

The real coefficients  $a_{ij}$  are determined, up to multiplicative constants, by replacing (4) into the transmission conditions in (1). Defining  $\rho_0 := \frac{1-pH}{1+pH}$ , there are two simple eigenvalues (see Figure 3 for the corresponding eigenfunctions)

$$\lambda = \rho_0, \mathbf{a} = a(1, 1, 1, 1), \quad \lambda = -\rho_0, \mathbf{a} = a(1, -1, -1, 1), \quad a \in \mathbb{R} \setminus 0.$$

Note that  $pH = 1$  is the only case where  $\mathcal{T}$  has a kernel.

### 3.2 Cross-point case: exponential modes

In the case with a cross-point (see Figure 1 middle), there are also exponential modes,  $\mathbf{U}(x, y, \zeta, \mathbf{a})$  with  $\zeta \in \mathbb{C} \setminus 0$ , defined in the subdomains by

$$\begin{aligned} u_{11} &= a_{11} \sin \zeta(x+H) \sinh \zeta(y-H), & u_{12} &= a_{12} \sin \zeta(x-H) \sinh \zeta(y-H), \\ u_{21} &= a_{21} \sin \zeta(x+H) \sinh \zeta(y+H), & u_{22} &= a_{22} \sin \zeta(x-H) \sinh \zeta(y+H). \end{aligned} \quad (5)$$

The transmission conditions in (1) give  $\lambda^2 = \rho(\zeta; p)^2$ , where  $\zeta$  is solution of the dispersion equation  $\rho(\zeta; p)^2 = \rho_h(\zeta, p)^2$  with

$$\rho(\zeta; p) := \frac{\zeta \cos \zeta H - p \sin \zeta H}{\zeta \cos \zeta H + p \sin \zeta H}, \quad \rho_h(\zeta; p) := \frac{\zeta \cosh \zeta H - p \sinh \zeta H}{\zeta \cosh \zeta H + p \sinh \zeta H}. \quad (6)$$

By the symmetry of the problem, changing  $\zeta$  into  $i\zeta$  corresponds to changing  $x$  into  $y$ . For each  $\lambda$ , there is an eigenspace of dimension 2, corresponding to  $\zeta$  and  $i\zeta$ , giving rise to two types of modes:

Type 1:  $\rho(\zeta; p) = \rho_h(\zeta, p)$ , with eigenvalues and eigenfunctions of subtype

$$\begin{aligned} 1.1 : \quad & \lambda = \rho_h(\zeta; p), \quad \mathbf{a}(\zeta) = \mathbf{a}(i\zeta) = (1, 1, 1, 1), \\ 1.2 : \quad & \lambda = -\rho_h(\zeta; p), \quad \mathbf{a}(\zeta) = \mathbf{a}(i\zeta) = (1, -1, -1, 1) \end{aligned}$$

Type 2:  $\rho(\zeta; p) = -\rho_h(\zeta, p)$ , with eigenvalues and eigenfunctions of subtype

$$\begin{aligned} 2.1 : \quad & \lambda = \rho_h(\zeta; p), \quad \begin{cases} \mathbf{a}(\zeta) = (1, -1, 1, -1), \\ \mathbf{a}(i\zeta) = (1, 1, -1, -1), \end{cases} \\ 2.2 : \quad & \lambda = -\rho_h(\zeta; p), \quad \begin{cases} \mathbf{a}(\zeta) = (1, 1, -1, -1), \\ \mathbf{a}(i\zeta) = (1, -1, 1, -1). \end{cases} \end{aligned}$$

Note that all eigenvalues satisfy  $|\lambda| < 1$ , and if  $\zeta$  is a solution, then also  $-\zeta, i\zeta, -i\zeta$  are solutions. So the following Theorems only characterize the solutions  $\zeta$  in the quarter plane defined by  $Q = \{\operatorname{Re} \zeta \geq 0, \operatorname{Im} \zeta > 0\}$ .

**Theorem 1 (Type 1)**  $\rho = \rho_h \iff \tan \zeta H = \tanh \zeta H$ , whose solutions  $\zeta$  in  $Q$  form a sequence  $\zeta_k^1$ , with  $\zeta_0^1 = 0$ , and  $\zeta_k^1 H \sim (k + \frac{1}{4})\pi - e^{-2k\pi}$  for  $k$  large.

**Theorem 2 (Type 2)**  $\rho = -\rho_h \iff p^2 \tan \zeta H \tanh \zeta H = \zeta^2$ , whose solutions  $\zeta$  in  $Q$  form a sequence  $\zeta_k^2$ , with  $\zeta_k^2 \in \mathbb{R}_+^*$  for  $k \geq 1$ ,  $\zeta_k^2 H \sim (k + \frac{1}{2})\pi - (\frac{pH}{k\pi})^2$  for  $k \geq 1$ , and  $\zeta_0 = (1+i)\zeta_d$ ,  $\zeta_d \in \mathbb{R}$  for  $p > 1$ ,  $\zeta_0 \in (0, \frac{\pi}{2})$  for  $p \leq 1$ .

These results are obtained by classical analysis, the little Picard Theorem and the Rouché Theorem, see for instance [8]. Furthermore, let  $V = \{f \in H^1(0, \pi), f(0) = 0\}$ ; then, by complex analysis, in particular nonharmonic Fourier series, see [10, 3], we can prove with  $\xi = \zeta \frac{H}{\pi}$ :

**Theorem 3 (Completeness)** The  $\sin(\xi_k^1 x)$  are a complete family in  $V$ , the  $\sin(\xi_k^2 x)$  form a Riesz basis in  $V$  (when  $p > 1$ , for  $k = 0$  take real and imaginary parts).

## 4 Interface operators

The  $\zeta_k$  defined above are used to define the trace of the eigenfunctions. Consider for instance the north west subdomain  $\Omega_{11}$ , and map  $\partial \Omega_{11}$  to  $(0, \pi) \times (0, \pi)$  as indicated in Figure 4, which maps the trace of the basis function  $(-\sinh \zeta H \sin \zeta(x+H), \sin \zeta H \sinh \zeta(y-H))$  to  $(\sinh \xi \pi \sin \xi x, \sin \xi \pi \sinh \xi x)$ . We already have density results of the  $\sin \xi x$  in  $V$ , but we must extend these results to the mixed traces in Figure 4 in  $W = \{(f, g) \in V \times V, f(\pi) = g(\pi)\}$ . Define

$$\varphi_k^j = \frac{\sin \xi_k^j x}{\xi_k^j \sin \xi_k^j \pi}, \quad \psi_k^j = \frac{\sinh \xi_k^j x}{\xi \sinh \xi_k^j \pi}, \quad \mathcal{A}^j \varphi_k^j = \psi_k^j, k = 0, \dots$$

It is crucial to define this properly and give the properties of  $\mathcal{A}^j$ . By density the definition above will allow us to define each of the  $\mathcal{A}^j$  on  $V$ , and then to combine in

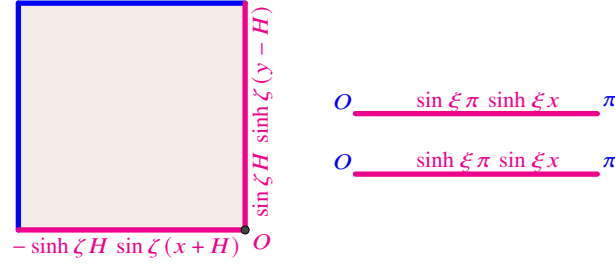


**Fig. 4** Mapping of the traces for the top left subdomain  $\Omega_{11}$ .

$W$  into  $\mathcal{B}^j(f, g) = (f + \mathcal{A}^j g, g + \mathcal{A}^j f)$ . We can first extend the results in Theorem 3:

**Theorem 4** *The family  $\{\varphi_k^1\}$  is a Schauder basis in  $V$ . Consequently the operator  $\mathcal{A}^1$  extends to a linear bounded operator with norm smaller than or equal to 1. It is furthermore self-adjoint.*

**Idea of the proof.** To pass from complete to Schauder, we use the dispersion equation for the family of Type I in Theorem 1 to compare  $(\varphi_n, \varphi_k)$  and  $(\psi_n, \psi_k)$  in the semi  $H^1$  norm. A frame inequality then follows for the set of  $\varphi_k$  minus the affine function  $\varphi_0$ , and we then complete the proof by approximation and orthogonalization. This result is crucial to to prove finally the density result for the first family:

**Theorem 5** *The range of  $\mathcal{B}^1$  is dense in  $W$ .*

The proof uses the equivalence with the fact that the orthogonal of the adjoint is zero. For the moment we have a partial result on  $\mathcal{B}^2$ :

**Theorem 6** *For  $p \leq 1$ , the range of  $\mathcal{B}^2$  is dense in  $W$ .*

The proof relies on precise estimates on the norm of  $\mathcal{A}^2$ . We have no proof yet for  $p > 1$ , but we have numerical evidence for the estimates.

## 5 Back to the operator $\mathcal{T}$ and its spectrum

Recombining and counting the traces in the subdomains, we obtain

**Theorem 7** *For  $p < 1$ , the traces of the eigenmodes of  $\mathcal{T}$  on the skeleton  $S = \coprod \partial\Omega_{ij}$  are a complete system in  $\mathbb{U}$ .*

Let us conclude now on the spectrum. For the fundamental results in functional analysis that we use, see [1]. The spectrum  $\sigma(\mathcal{T})$  of  $\mathcal{T}$  is the set of complex numbers  $\lambda$  such that  $\mathcal{T} - \lambda I$  does not have a bounded inverse. Since  $\mathcal{T}$  is a bounded operator on  $\mathbb{U}$ , the open mapping theorem implies that if  $\mathcal{T} - \lambda I$  is bijective, the inverse is bounded. Therefore the spectrum is the set of complex numbers  $\lambda$  such that  $\mathcal{T} - \lambda I$  is not a bijection. The spectrum of  $\mathcal{T}$  is a compact subset of the disk of center 0 and radius  $\|\mathcal{T}\|$ . The spectrum consists of three parts.

- The point spectrum  $\sigma_p(\mathcal{T})$  is the set of  $\lambda \in \sigma(\mathcal{T})$  such that  $\mathcal{T} - \lambda I$  is not injective.
- The continuous spectrum  $\sigma_c$  is the set of  $\lambda \in \sigma(\mathcal{T})$  such that  $\mathcal{T} - \lambda I$  is injective with dense range.
- The residual spectrum  $\sigma_r$  is the set of  $\lambda \in \sigma(\mathcal{T})$  such that  $\mathcal{T} - \lambda I$  is injective but its range is not dense.

We have now all elements to provide an almost complete description of the spectrum:

**Theorem 8**

1.  $\pm 1 \in \sigma(\mathcal{T})$ .
2. All the eigenvalues  $\lambda_k^{\pm, j} = \pm \rho_h(\zeta_k^j, p)$  obtained by separation of variables from the  $\zeta_k^j$  in Section 3 belong to the point spectrum.
3. There is no residual spectrum.

If moreover the family of eigenvectors  $\mathbf{U}_k^{\pm, j} = \mathbf{U}(x, y, \zeta_k^j, \mathbf{a}^{\pm, j})$  obtained by separation of variables in Section 3.2 is a Schauder basis, then

4. there is no other eigenvalue than the  $\lambda_k^{\pm, j}$ .
5.  $\sigma_c(\mathcal{T}) = \{\pm 1\}$ .

To conclude, we show for  $p = 4$  the first real modes of type 1 and 2 in Figures 5 and 6, and the diagonal mode in Figure 7, where the eigenvalues are purely imaginary.

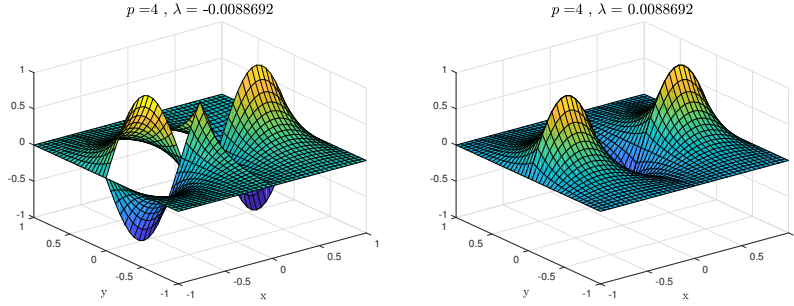


**Fig. 5** View of the first mode of type 1,  $\zeta = 3.9266$

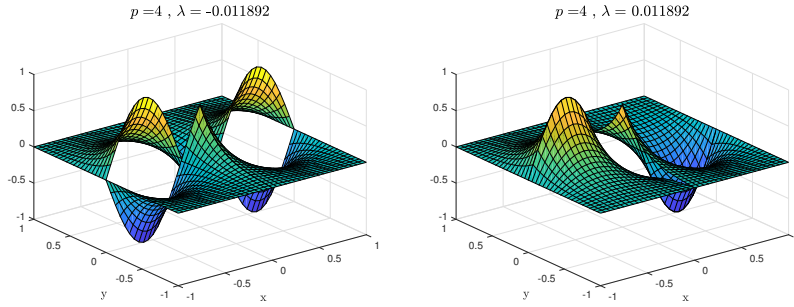


**Fig. 6** View of the first real modes of type 2,  $\zeta = 3.9028$

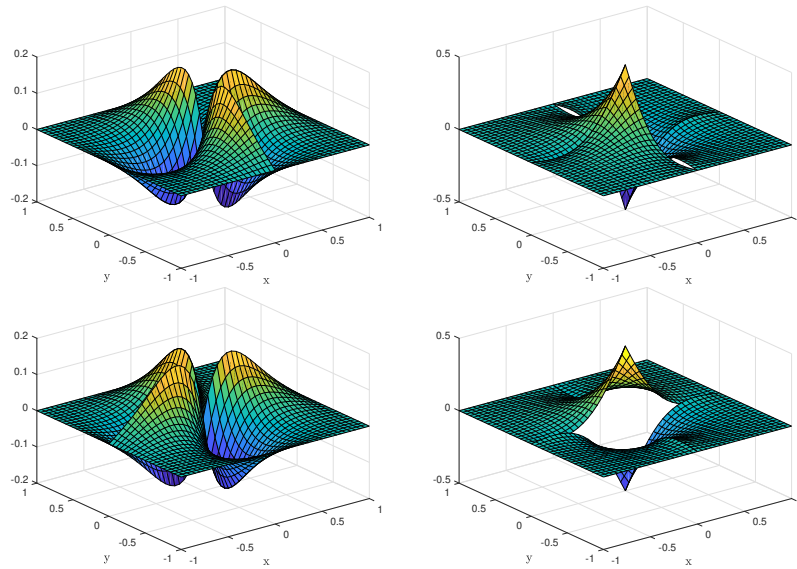


**Fig. 7** View of the first modes of type 2 on the diagonal  $\zeta = (1 + i)2.8123$ . Top:  $\lambda = -0.41i$ . Bottom  $\lambda = 0.41i$ . Left: real part. Right: imaginary part.

## References

1. Brezis, H.: Functional analysis, Sobolev spaces and partial differential equations. Springer (2011)
2. Cuvelier, F., Gander, M.J., Halpern, L.: Fundamental coarse space components for Schwarz methods with crosspoints. In: Domain Decomposition Methods in Science and Engineering XXVI, pp. 29–50. Springer (2022)
3. Cuvelier, F., Gander, M.J., Halpern, L.: Modal analysis of the Robin-Schwarz operator. In preparation (2035)
4. Gander, M.J.: Schwarz methods over the course of time. *Electron. Trans. Numer. Anal* **31**(5), 228–255 (2008)
5. Gander, M.J., Halpern, L., Santugini-Repique, K.: Continuous analysis of the additive Schwarz method: a stable decomposition in H1. *ESAIM Mathematical Modelling and Numerical Analysis* **49**(3), 365–385 (2011)
6. Lions, P.L.: On the Schwarz alternating method. I. In: First international symposium on domain decomposition methods for partial differential equations, vol. 1, p. 42. Paris, France (1988)
7. Lions, P.L.: On the Schwarz alternating method III: A variant for nonoverlapping subdomains. In: T.F. Chan, R. Glowinski, J. Périaux, O. Widlund (eds.) Third International Symposium on Domain Decomposition Methods for Partial Differential Equations, held in Houston, Texas, March 20–22, 1989, pp. 202–223. SIAM, Philadelphia, PA (1990)
8. Rudin, W.: Real and complex analysis. McGraw-Hill (1987)
9. Saad, Y.: Iterative methods for sparse linear systems. SIAM (2003)
10. Young, R.M.: An introduction to nonharmonic Fourier series, revised edition. Academic Press (2001)